membranes

MDPI

Article

A Simplified Kinetic Modeling of CO_2 Absorption into Water and Monoethanolamine Solution in Hollow-Fiber Membrane Contactors

Mai Lien Tran [1,†], Chi Hieu Nguyen [1,†], Kuan-Yan Chu [2] and Ruey-Shin Juang [2,3,4,*]

[1] Institute of Environmental Science, Engineering and Management, Industrial University of Ho Chi Minh City, Ho Chi Minh City 700000, Vietnam; tranmailien@iuh.edu.vn (M.L.T.); nguyenchihieu_mt@iuh.edu.vn (C.H.N.)
[2] Department of Chemical and Materials Engineering, Chang Gung University, Guishan, Taoyuan 33302, Taiwan; s955244@mail.yzu.edu.tw
[3] Department of Internal Medicine, Division of Nephrology, Chang Gung Memorial Hospital Linkou, Taoyuan 33305, Taiwan
[4] Department of Safety, Health and Environmental Engineering, Ming Chi University of Technology, Taishan, New Taipei City 24301, Taiwan
* Correspondence: rsjuang@mail.cgu.edu.tw
† These authors contributed equally to this work.

Abstract: The absorption of CO_2 from CO_2-N_2 gas mixtures using water and monoethanolamine (MEA) solution in polypropylene (PP) hollow-fiber membrane contactors was experimentally and theoretically examined. Gas was flowed through the lumen of the module, whereas the absorbent liquid was passed counter-currently across the shell. Experiments were carried out under various gas- and liquid-phase velocities as well as MEA concentrations. The effect of pressure difference between the gas and liquid phases on the flux of CO_2 absorption in the range of 15–85 kPa was also investigated. A simplified mass balance model that considers non-wetting mode as well as adopts the overall mass-transfer coefficient evaluated from absorption experiments was proposed to follow the present physical and chemical absorption processes. This simplified model allowed us to predict the effective length of the fiber for CO_2 absorption, which is crucial in selecting and designing membrane contactors for this purpose. Finally, the significance of membrane wetting could be highlighted by this model while using high concentrations of MEA in the chemical absorption process.

Keywords: kinetic modeling; CO_2 absorption; monoethanolamine; hollow-fiber membrane contactors

Citation: Tran, M.L.; Nguyen, C.H.; Chu, K.-Y.; Juang, R.-S. A Simplified Kinetic Modeling of CO_2 Absorption into Water and Monoethanolamine Solution in Hollow-Fiber Membrane Contactors. *Membranes* **2023**, *13*, 494. https://doi.org/10.3390/membranes13050494

Academic Editors: Antonia Pérez de los Ríos and Alan D. Pérez

Received: 8 April 2023
Revised: 1 May 2023
Accepted: 4 May 2023
Published: 5 May 2023

1. Introduction

Carbon dioxide has been proven to be the largest contribution of greenhouse gases, which results in the increase in the earth's surface temperature. It is also reported that half of CO_2 emissions are produced by power plants using fossil fuels [1–3]. Hence, the development of an efficient separation process is highly desired to remove CO_2 from the places where CO_2 is generated. In general, the bubble column, packed tower, venturi scrubber, and sieve tray column can be used for this purpose. The commercial process that is widely used for CO_2 separation is the packed column, but new technology is still required because the packed towers, for example, have many advantages such as channeling, flooding, and large-scale equipment. The gas absorption process using membrane units is considered as an alternative to recover CO_2 from waste gas streams. The hollow-fiber membrane contactor (HFMC) offers a much larger contact area per unit volume in comparison with packed and tray columns and has the advantages of no entrainment, no foaming, and no restrictions on operating flow rates [2–9].

Alkanolamines including monoethanolamine (MEA), dithenaolamine (DEA), *N*-methyl-diethanolamine (MDEA), di-2-propanolamine, and 2-amino-2-methyl-l-propanol

(AMP) are dominantly used as absorbent liquids for CO_2 removal due to their high reaction rates [10–14]. Using HFMCs, Yeon et al. [15] have examined the absorption of CO_2 in PVDF and PTFE modules using single MEA absorbent. Wang et al. [16] have theoretically studied the capture of CO_2 by three solutions of MDEA, AMP, and DEA in HFMCs with a non-wetting mode. In addition, Yeon et al. [17] have examined the rate of CO_2 absorption in PP module using the mixed absorbent liquids of piperazine (PZ) and triethanolamine (TEA).

Various kinetic models have been developed in the literature to follow the absorption of CO_2 in HFMCs by absorbent liquids [8,9,15,16,18–27]. Most of them have used the complicated numerical methods to solve a set of differential mass balance equations to predict the change of CO_2 concentration along the hollow fibers. For example, Kim and Yang [18] have adopted a set of governing equations with common assumptions that the velocity in the lumen side can be described as fully developed parabolic profile and that the velocity through the shell side can be characterized by the free surface model of Happel [26]. Yeon et al. [15] have also employed differential mass balance equations to describe diffusion and forced convection in a medium that flows laminarly in the lumen side. They have assumed an irreversible reaction of CO_2 taking place with MEA and determined the mass transfer rates of CO_2 in PVDF and PTFE hollow fibers. Generally speaking, the mathematical complexity of numerical methods used for solving a set of differential mass balance equations makes the kinetic model somewhat practically inconvenient.

The absorption of CO_2 from a synthetic 15 vol% CO_2-N_2 gas mixture by using water and MEA solutions was investigated in HFMCs. The effects of liquid- and gas-phase velocities as well as the pressure difference between liquid and gas phases on the flux of CO_2 absorption were explored. A simplified model involving mass balance equations-only was proposed to follow the absorption process of CO_2 and to estimate the effective length of the fiber, in which the non-wetting mode was assumed and the overall mass-transfer coefficient based on physical and chemical absorption was considered.

2. Kinetic Modeling

2.1. Determination of Overall Mass-Transfer Coefficient

The mass transfer between gas and liquid phases through HFMC occurs in three parts: stagnant gas film, the membrane itself, and stagnant liquid film [15]. The overall rate of CO_2 absorption, R_A (mol s^{-1}), is expressed by Equation (1):

$$R_A = K_L A_T \Delta C_{lm} = Q_g \left(C_{g,out} - C_{g,in} \right) \quad (1)$$

where K_L is the overall mass-transfer coefficient based on liquid phase (m s^{-1}); A_T is the effective contact area (m^2); Q_L is the volumetric flow rate of liquid phase (m^3 s^{-1}); and $C_{g,out}$ and $C_{g,in}$ are the gas-phase concentrations of CO_2 in the outlet and inlet of the module, respectively (mol m^{-3}). Additionally, ΔC_{lm} is the logarithmic mean concentration difference, which is expressed by the following equation:

$$\Delta C_{lm} = \frac{\left(HC_{g,in} - C_{L,out} \right) - \left(HC_{g,out} - C_{L,in} \right)}{ln\left[\left(HC_{g,in} - C_{L,out} \right) / \left(HC_{g,out} - C_{L,in} \right) \right]} \quad (2)$$

Here, the value of H for CO_2 in water is adopted to be 2.916 kPa m^3 mol^{-1} [28], whereas it is taken to be 3.564 kPa m^3 mol^{-1} in 0.005–0.01 M of MEA solution and becomes 3.518 kPa m^3 mol^{-1} in 1.0 M of MEA solution [29].

2.2. Model Development

A simplified mathematical model was developed based on the mass balance concept, combining process conditions, membrane properties, and module geometric characteristics. The following assumptions are made: (a) absorption of single component (CO_2) from a CO_2-N_2 gas mixture flowing through the lumen side of the module into an aqueous solution flowing in the shell side; (b) steady state and isothermal operation; (c) Newtonian

fluids with constant physical properties; (d) hydrophobic membrane with non-wetting; and (e) the applicability of Henry's law [8,9,18,19,21,22,25–27].

As shown in Figure 1, the mass balance of CO_2 within the membrane contactor using water as absorbent liquid is described as follows:

$$Q_L C_{L,in} - Q_L C_{L,out} + J_A A_T = 0 \quad (3)$$

where J_A is the flux of CO_2 absorption through the hollow fibers (mol m^{-2} s^{-1}), which is calculated by the following equation:

$$J_A = K_L(C_{L,in} - C_{L,out}) \quad (4)$$

where C_L is the concentration of CO_2 in liquid phase (mol m^{-3}).

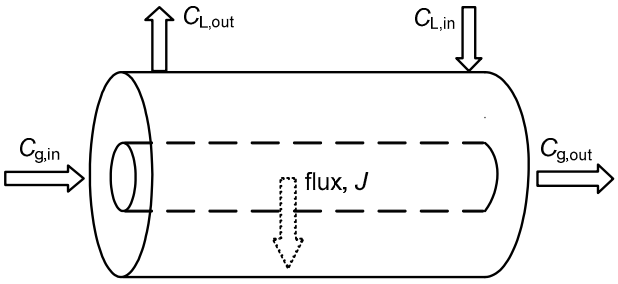

Figure 1. The control volume of gas absorption in hollow fibers.

Since J_A depends on the concentration of CO_2, it must be calculated every time according to Equations (3) and (4) using the MATLAB program (MathWorks, Natick, MA, USA). The number of grids (N_z) in the computational domain of 500 (in the axial direction) was used. Therefore, the value of $C_{L,out}$ can be calculated by Equation (5):

$$C_{L,out} = \frac{Q_L C_{L,in} + K_L(A_T/N_z)C_{g,in}}{Q_L + K_L(A_T/N_z)} \quad (5)$$

On the other hand, the mass balance within the membrane contactor using MEA solution as absorbent liquid is described as follows:

$$Q_L C_{L,in} - Q_L C_{L,out} + J_A A_T - r_A V_{shell} = 0 \quad (6)$$

where r_A is the reaction rate between MEA and CO_2 (mol m^{-3} s^{-1}).

In general, carbamate is formed when CO_2 gas reacts with primary and secondary alkanolamines [13,30,31]:

$$CO_2 + 2R_1R_2NH \rightleftharpoons R_1R_2NCO_2^- + R_1R_2NH_2^+ \quad (7)$$

where R_1 is an alkyl group, and R_2 is H for primary amines and an alkyl group for secondary amines. The zwitterion mechanism has been commonly used in aqueous alkanolamine solutions [32,33]. The reaction steps successively involve the formation of a zwitterion,

$$R_1R_2NH + CO_2 \rightleftharpoons R_1R_2NH^+CO_2^-,\ k_{2,amine}/k_{-1} \quad (8)$$

and the subsequent removal of the proton by a base B (base catalysis),

$$R_1R_2NH^+CO_2^- + B \xrightarrow{k_B} R_1R_2NCO_2^- + BH^+ \quad (9)$$

where B could be an amine, OH^-, or H_2O, although the contribution of OH^- can be neglected because its concentration is very low, compared to that of the amine and H_2O [14].

According to this zwitterion mechanism, the forward reaction rate equation for CO_2 at quasi-steady state, r_A, has been derived by Danckwerts [34] as follows:

$$r_A = \sum \frac{k_{2,amine} C_L C_{amine}}{1 + \{[(k_w/k_{-1})C_w] + \sum[(k_{amine}/k_{-1})C_{amine}]\}^{-1}} \quad (10)$$

So, in the MEA-CO_2 system we have

$$r_A = \sum \frac{k_{2,MEA} C_L C_{MEA}}{1 + \{[(k_w/k_{-1})C_w] + [(k_{MEA}/k_{-1})C_{MEA}]\}^{-1}} \quad (11)$$

where C_w is equal to 55.5 M. The kinetic parameters of $k_{2,MEA}$, (k_w/k_{-1}), and (k_{MEA}/k_{-1}) adopted here at 25 °C are 6.358 m^3 mol^{-1} s^{-1}, 1.507 × 10^{-6} m^3 mol^{-1}, and 2.485 × 10^{-4} m^3 mol^{-1}, respectively [13,25]. In this case, the value of $C_{L,out}$ can be calculated by Equation (12):

$$C_{L,out} = \frac{Q_L C_{L,in} + K_L(A_T/N_z)C_{g,in} - r_A(V_{shell}/N_z)}{Q_L + K_L(A_T/N_z)} \quad (12)$$

3. Materials and Methods

3.1. Materials

MEA was purchased from Aldrich Chemicals Co. A Liqui-Cel microporous hollow-fiber extra-flow 2.5 × 8 module, which was supplied from3M^{TM} Separation and Purification Division. (Charlotte, NC, USA), was used as membrane contactor for CO_2 absorption in this work. The hollow fibers in this module were X-50 type and made of polypropylene (PP). The characteristics of the membrane contactor are listed in Table 1. Deionized water (Millipore, Milli-Q, Burlington, MA, USA) was used. All chemicals were used without any further purification.

Table 1. Characteristics of HFMCs used in this work (Hoechst Celanese Liqui-Cel extra-flow model with central baffle).

Description	Extra-Flow 2.5 × 8 Module	Extra-Flow 4 × 28 Module
Shell material	Polypropylene	Polypropylene
Shell length (mm)	203	704
Shell outer diameter (mm)	77	127
Shell inner diameter (mm)	63	111
Shell hydraulic diameter (mm)	4.7	-
Fiber material	Celgard X-50 polypropylene	Celgard X-50 polypropylene
Number of fibers	~10,200	-
Fiber length, L (mm)	190	620
Fiber inner diameter (μm)	220	220
Fiber outer diameter (μm)	300	300
Fiber membrane surface area, A_T (m^2)	1.4	20
Fiber membrane pore size (μm)	0.04	0.04
Fiber membrane porosity	0.4	0.4
Effective area/volume (cm^2 cm^{-3})	25.5	36.4

3.2. Absorption Experiments

The experimental setup for CO_2 removal is schematically illustrated in Figure 2. The gas containing 15 vol% of CO_2 (balance N_2) was passed upstream in the lumen side of the module, and the absorbent liquid was supplied downstream in the shell side. The absorbent liquids used in this study were deionized water and the aqueous solution containing 0.005–1.0 M MEA, which had a volume of 1 L otherwise stated elsewhere. The gas-phase velocity u_g was varied in the range of 0.041–0.124 m s^{-1}, and the liquid-phase

velocity u_L changed in the range of 0.008–0.02 m s^{-1}. The pressure difference of the liquid and gas phases was changed in the range of 15–85 kPa by a needle valve to form the stable gas-liquid interface within the module. The gases coming from the absorption were sampled and analyzed by TCD-GC (Shimadzu, GC-14B, Kyoto, Japan) at pre-set time intervals. After each run, the deionized water (2 dm^3) was poured into both sides of the membrane contactor to remove the absorbent liquids. Then, ethanol (0.5 dm^3) was flowed through both sides of the module to remove water in the pores of the membrane. Finally, N_2 gas went through both sides of the module for 30 min.

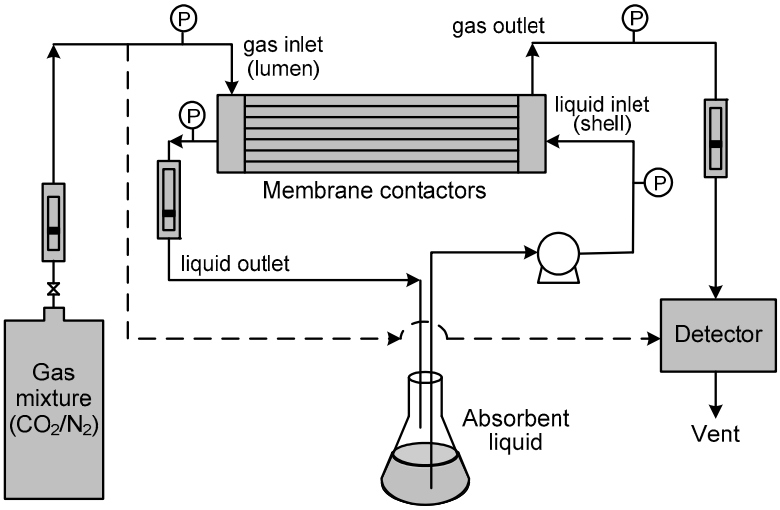

Figure 2. Experimental setup of CO_2 absorption in Liqui-Cel extra-flow model HFMCs.

4. Results and Discussion

4.1. Effect of Fluid Velocity on K_L without Absorbent Recycling

The measured changes of CO_2 concentrations in both phases between the inlet and outlet of the module were used for the calculation of the rates of CO_2 absorption R_A and the overall mass-transfer coefficients K_L by Equation (1). Figures 3 and 4 show the influences of fluid velocities on the K_L values in PP hollow fibers using water and 0.005 M of MEA solution as absorbent liquids. As expected, K_L increases initially with increasing gas-phase velocity u_g but then decreases (Figure 3). The decreased K_L is likely because the retention time of gas reduces when u_g is increased. It is noted that the flux of CO_2 absorption, J_A, at higher u_g is still larger than that at low u_g. On the other hand, the K_L value always increases with increasing liquid-phase velocity u_L using both water and MEA solutions as absorbent liquids as shown in Figure 4. Furthermore, the influence of gas-phase flow rate in chemical absorption (i.e., MEA) is more significant than that in physical absorption (i.e., water).

Yeon et al. [15] have ever investigated the absorption of CO_2 in PVDF and PTFE hollow fiber modules using single MEA solution. They also found that the flux of CO_2 increases with an increase in liquid-phase velocity, and that initially increases with an increase in gas-phase velocity. However, it has been reported according to theoretical analysis that the flux of CO_2 absorption by MDEA solution is virtually unaffected by liquid-phase velocity [16]. This is likely due to the variations of membrane configuration and the range of gas-phase velocity. Under the present conditions studied, the difference of K_L scales by 8 times between the systems using water and MEA solution is due to the characteristics of physical and chemical absorption.

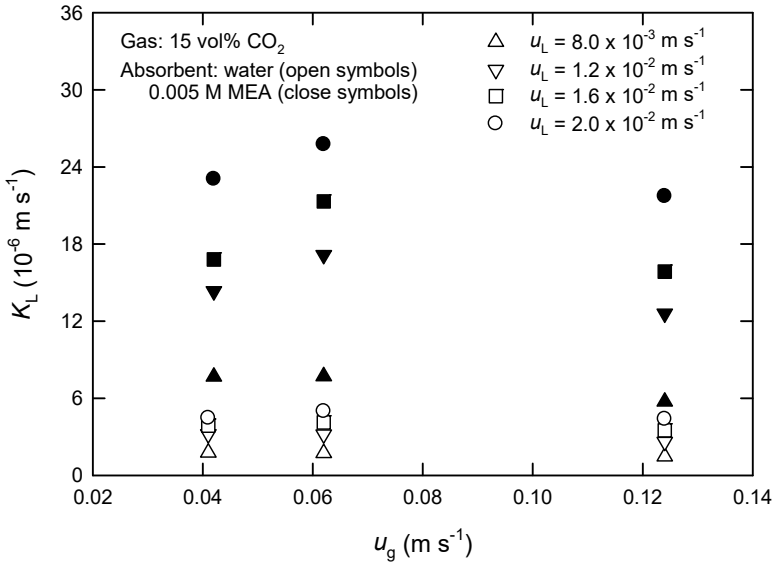

Figure 3. The overall mass-transfer coefficient at various gas-phase velocities using water and 0.005 M of MEA solution as absorbent liquids in extra-flow 2.5 × 8 module.

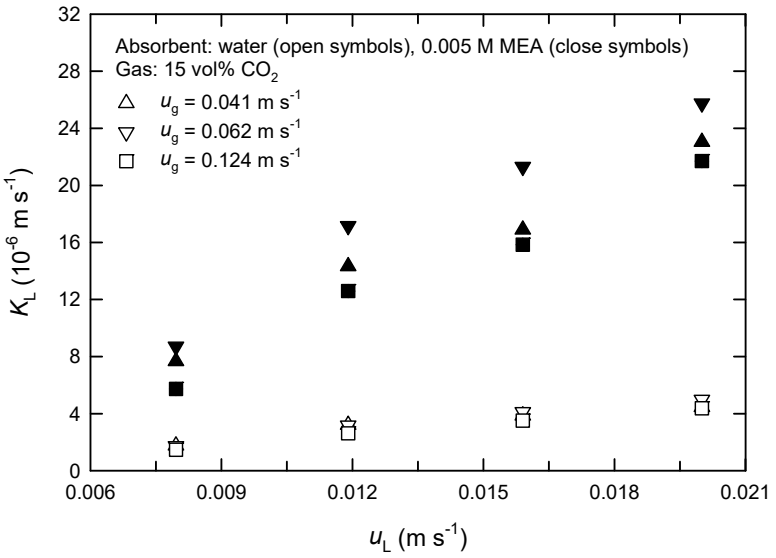

Figure 4. The overall mass-transfer coefficient at various liquid-phase velocities using water and 0.005 M of MEA solution as absorbent liquids in extra-flow 2.5 × 8 module.

It is expected that the experimental K_L values evaluated by Equation (1) should vary with MEA concentration in chemical absorption processes. This fact makes the proposed kinetic model, Equation (12), rather complicated and practically unpromising. For simplicity, accordingly, the value of K_L evaluated from the physical absorption process is applied throughout this work for model predictions, regardless of physical or chemical absorption processes.

4.2. Effect of Operation Parameters on CO_2 Removal with Absorbent Recycling

The time changes of the concentrations of CO_2 in the outlet of the module under various gas- and liquid-phase velocities using different absorbent liquids are shown in Figures 5 and 6. At a specific time (that is, a specific position along the axial direction in HFMCs), the steady state is assumed to be calculated J_A from Equations (3) and (4) in the case of using water as well as Equations (6) and (11) in the case of using MEA solution using the MATLAB program. Then, we can calculate the exit concentrations of CO_2 in the water

and MEA solution, $C_{L,out}$ by Equations (5) and (12), respectively. The exit concentration of CO_2 in the gas can obtained using Henry's law, $P_{g,out} = C_{L,out} \times H$, and ideal gas law. At the next time, similar procedures are repeated. Consequently, we can obtain the modeled results of $C_{g,out}$ at different times.

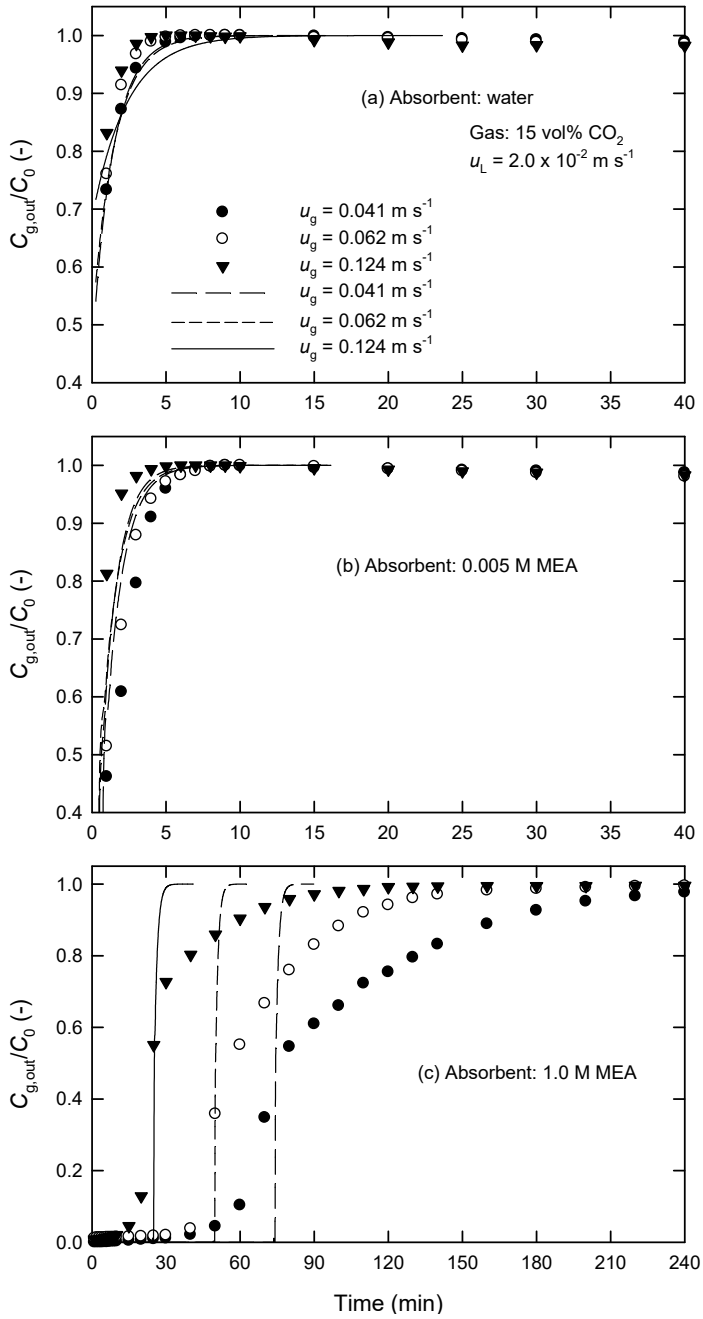

Figure 5. Effect of gas-phase velocity on the time changes of $C_{g,out}/C_0$ at $u_L = 2.0 \times 10^{-2}$ m s^{-1} using (**a**) water, (**b**) 0.005 M of MEA, and (**c**) 1.0 M of MEA as absorbent liquids in extra-flow 2.5 × 8 module (the solid and dashed curves are calculated by the proposed kinetic model).

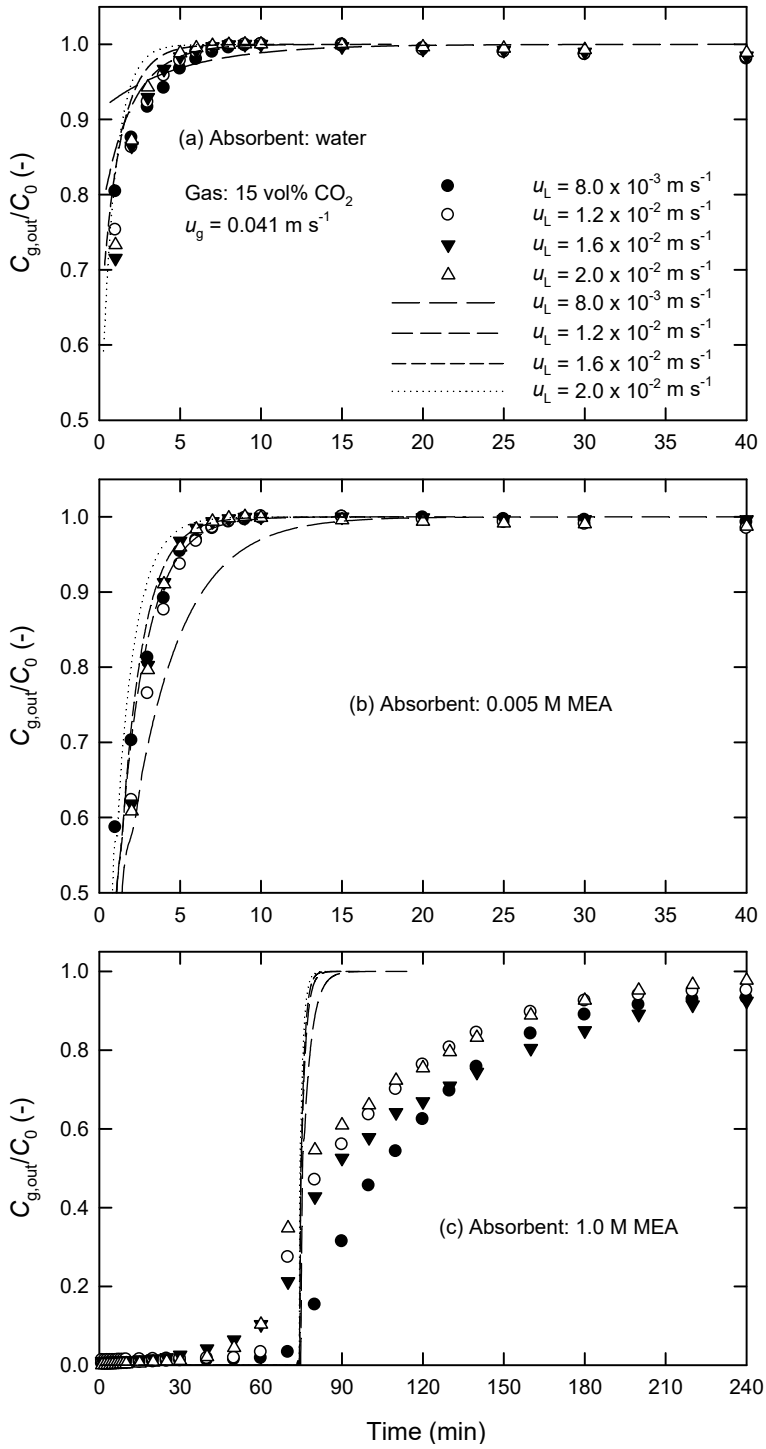

Figure 6. Effect of liquid-phase velocity on the time changes of $C_{g,out}/C_0$ at $u_g = 4.1 \times 10^{-2}$ m s^{-1} using (**a**) water, (**b**) 0.005 M of MEA, and (**c**) 1.0 M of MEA as absorbent liquids in extra-flow 2.5 × 8 module (the solid and dashed curves are calculated by the proposed kinetic model).

It is found that CO_2 can be removed by pure water only within 4 min, and the time elapsed when $C_{g,out}/C_0$ reaches unity becomes shorter with increasing u_g. It is expected that the absorption of CO_2 by recycling absorbent liquids is faster at a higher u_g. This phenomenon is more obvious in the case of aqueous MEA solution (Figure 5b,c). The time required when $C_{g,out} = C_0$ for MEA solution is much longer than that for water. This is because the CO_2 loading of the MEA solution, particularly at 1 M of MEA, is larger than that of water.

However, the effect of liquid-phase velocity u_L on CO_2 removal is not so apparent, as shown in Figure 6a,b. Figure 6c shows that the time required for $C_{g,out}$ to reach C_0 decreases with increasing u_L at high MEA concentrations, which is mainly a result of a larger mass-transfer coefficient at higher u_L. The loading of CO_2 of absorbent liquids is depleted more quickly when the rate of absorption increases. Furthermore, it is inferred that the resistance of liquid phase mass transfer is always important in chemical absorption, particularly at high MEA concentrations.

4.3. Validity of the Proposed Kinetic Model

Figures 5 and 6 also show the calculated results (solid and dashed curves) in the present PP hollow-fiber module. It is found that the measured results agree reasonably well with the calculated ones using water and low MEA concentrations as shown in Figures 5a,b and 6a,b. The standard deviation (SD) is less than 11% (mostly 7%), which is defined by

$$\mathrm{SD}(\%) = 100 \times \left\{ \sum_{N} \left[1 - \left(C_{\mathrm{calc}}/C_{\mathrm{expt}}\right)\right]^2/(N-1) \right\}^{1/2} \tag{13}$$

where the subscripts 'calc' and 'expt' are the calculated and measured values, respectively, and N is the number of data points. The agreement is also acceptable using 0.05 M of MEA solution, where SD is less than 15%. At higher MEA concentrations (e.g., 1.0 M of MEA in Figures 5c and 6c), the large SD (more than 100%) is likely attributed to the ignorance of membrane wetting effect in this model. However, the fact that the predicted lines still approximately pass through the "center of symmetry" of the measured curves, as shown in Figures 5c and 6c, can be understood by a uniform distribution of pore wetting within the membrane. Although the large SD values found in Figures 5c and 6c, this simple model would still reveal the time required for $C_{g,out}$ to reach $C_{0.}$

It is recognized that the wetting ratio of the membrane is a crucial factor on the mass transfer resistance during the absorption of gases in HFMCs. In general, the wetting ratio is dominantly affected by the pressure difference between the gas- and liquid-phases and hydrophobicity of absorbent. Experiments with various liquid-phase pressures P_L at a fixed gas-phase pressure (20 kPa) were also conducted in this work to understand such a factor on the rate of CO_2 absorption. It is found from Figure 7 that the effect of such pressure differences on CO_2 removal can be neglected using 0.005 M of MEA solution as absorbent liquid under the conditions investigated.

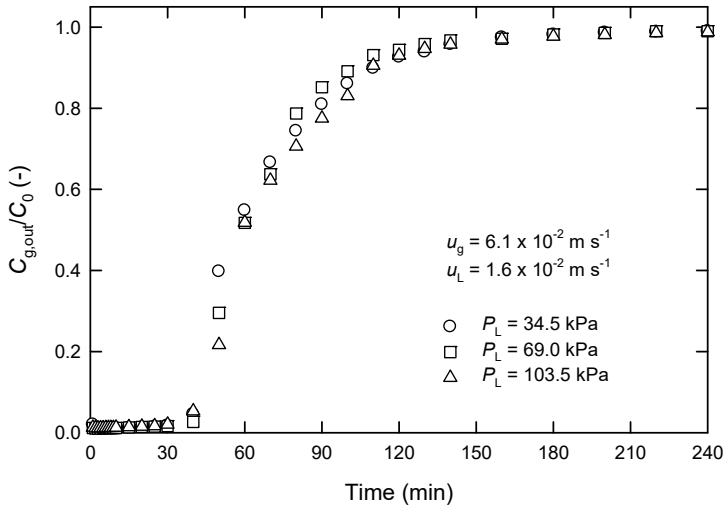

Figure 7. Effect of liquid-phase pressure in the shell of the module P_L on time changes of $C_{g,out}/C_0$ at a fixed gas-phase pressure of 20 kPa in extra-flow 2.5 × 8 module using 0.005 M of MEA as absorbent liquid.

It has been reported that neglecting axial diffusion will result in a much smaller CO_2 concentration along the length of the fiber and, thus, a higher rate of absorption. This is the case at low Peclet numbers ($=u_g L/D_{A,g}$), where $D_{A,g}$ is the diffusivity of CO_2 in gas phase ($= 1.51 \times 10^{-5}$ m^2 s^{-1}) [25]; However, such an effect becomes less when the Peclet number increases (for example, >50) [26]. In the present system, the axial diffusion plays a negligible role in kinetic modeling because the Peclet number is larger than 500.

Once the validity of the proposed simplified model was confirmed, an attempt was made to understand the role of the size of hollow fibers. Figure 8 shows the calculated results in a large HFMC, extra-flow 4 × 28 module (fiber length 620 mm, contact area 20 m^2, fiber inner diameter 0.22 mm), whose characteristics are listed in Table 1. In contrast to the case of extra-flow 2.5 × 8 module (fiber length 190 mm, contact area 1.4 m^2, fiber inner diameter 0.22 mm), the effect of u_L on the time required for $C_{g,out}$ reaching C_0 in a larger module is more significant (Figure 8a,b). It is noted that the volume of absorbent liquid was kept the same (14.3 L) in both modules. Moreover, the use of larger amount of absorbent liquid leads to a higher efficiency of CO_2 absorption, as compared in Figure 6b vs. Figures 8b and 6c vs. Figure 8c.

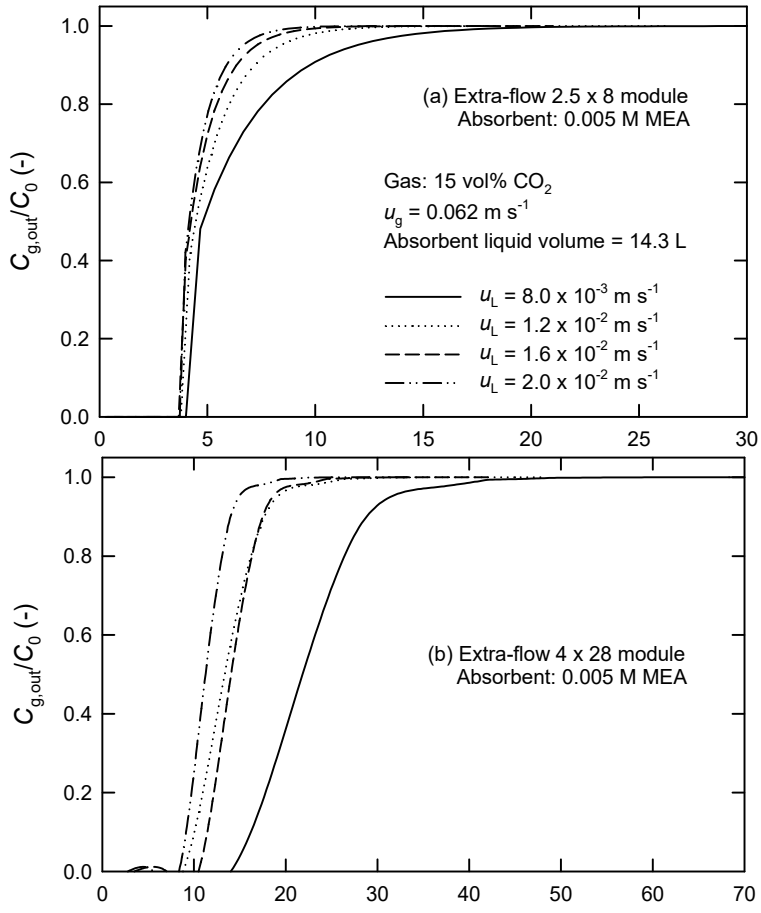

Figure 8. *Cont.*

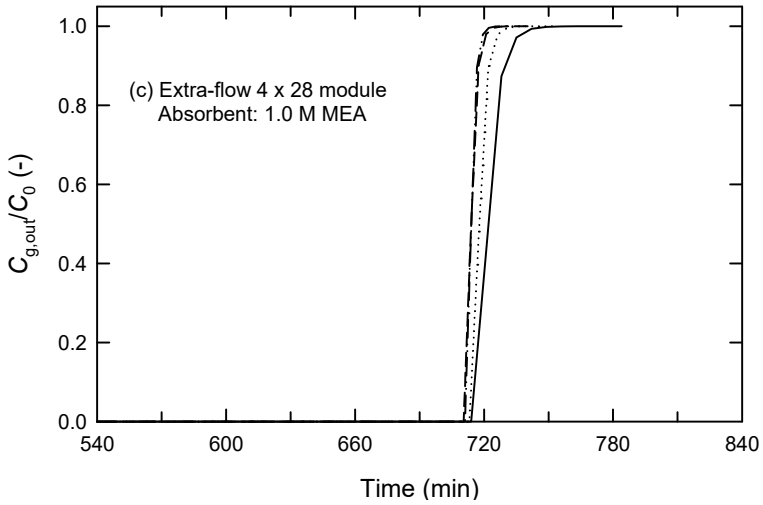

Figure 8. Effect of liquid-phase velocity on the time changes of $C_{g,out}/C_0$ at u_g = 0.062 m s^{-1} using (**a**) water, (**b**) 0.005 M of MEA, and (**c**) 1.0 M of MEA as absorbent liquids in extra-flow 2.5 × 8 and 4 × 28 modules.

Given the absence of experimental data using a larger extra-flow 4 × 28 module, this note is necessarily highly prospective. Additionally, smaller modules were used in the literature and in this work; they could deliver good agreement between the measured and predicted results.

4.4. Determination of Effective Fiber Length

On the other hand, the present model enables us to predict the concentration change of CO_2 along the fiber from the gas inlet to the outlet. It is found from Figure 9a,b that the CO_2 concentration in the outlet of the module, $C_{g,out}$, is higher when liquid-phase velocity u_L is smaller. In addition, $C_{g,out}$ becomes zero for all u_L values tested when u_g = 0.124 m s^{-1} using 0.05 M MEA solution as an absorbent liquid (Figure 9c). For example, the dimensionless length of the fiber (z/L) needed for nearly complete removal of 15% CO_2 is 0.2 (whereas z/L = 0.06 when C_g/C_0 = 0.01) using 0.05 M of MEA solution as u_g = 0.124 m s^{-1} and u_L = 2.0 × 10^{-2} m s^{-1}, as shown in Figure 9c. We call this the "effective" fiber length, L_{eff}. It is also found that L_{eff} remarkably reduces when more concentrated MEA solution is used as an absorbent liquid. Zhang et al. [27] have actually reported that CO_2 absorption by aqueous DEA solution in HFMC (Celgard MiniModule® 0.75 × 5 module, X-50 type fibers; fiber length 113 mm, contact area 0.09 m^2) is mainly conducted in the front segments near the inlet. For example, 20 vol% CO_2 in CO_2-N_2 mixture (u_g = 0.032 m s^{-1}) is mainly absorbed by 2 M of DEA (u_L = 0.15 m s^{-1}) in the segments up till z/L = 0.6 while CO_2 absorption is negligible in the rest of the segments. Although increasing u_g in the range 0.032–0.090 m s^{-1} can increase L_{eff}, approximately 20% of the total length has little absorption capacity. They thus concluded that increasing the length of the module is not an effective way to enhance CO_2 absorption when the module is longer than L_{eff}.

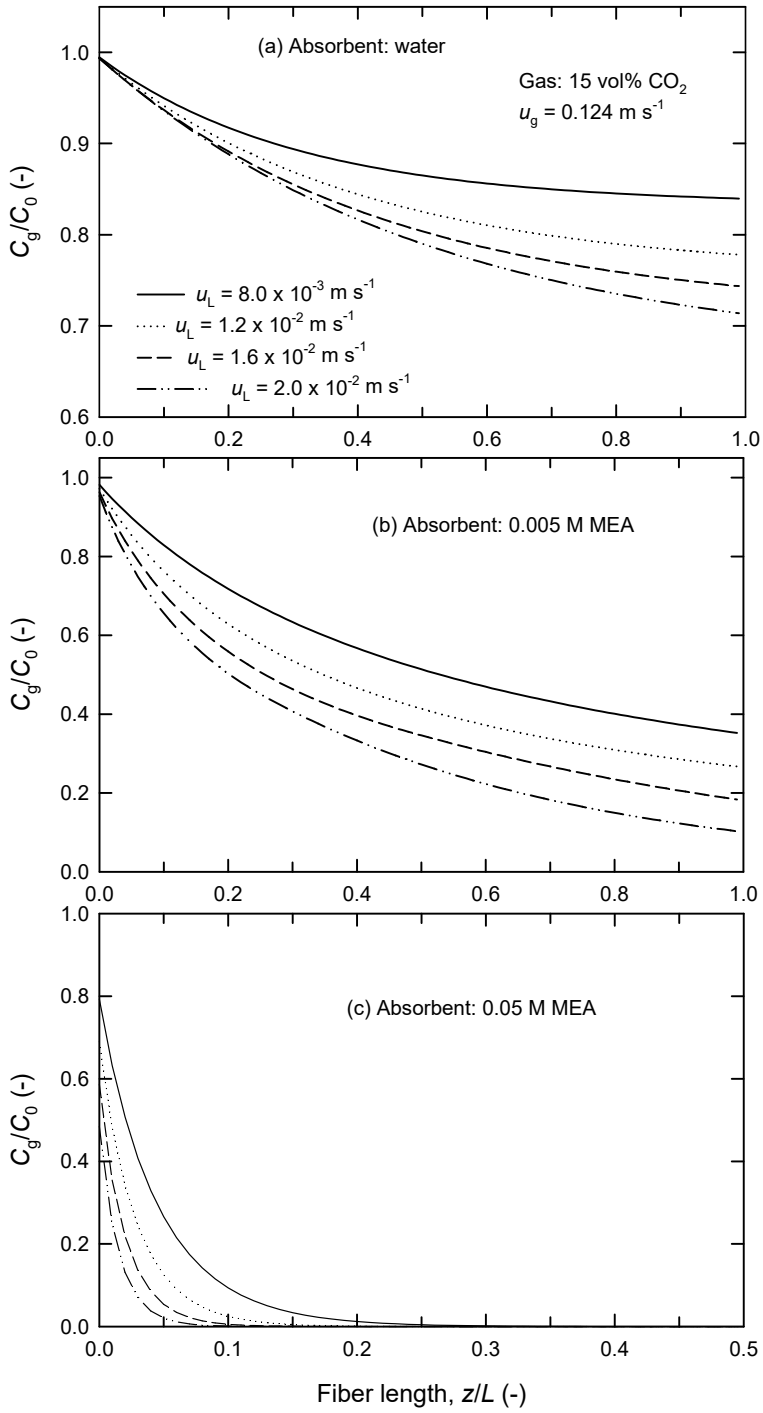

Figure 9. Effect of liquid-phase velocity on the variation of CO_2 removal along the length of the fiber at u_g = 0.124 m s^{-1} using (**a**) water, (**b**) 0.005 M of MEA, and (**c**) 0.05 M of MEA as absorbent liquids in extra-flow 2.5 × 8 module.

The calculated results of L_{eff} in extra-flow 2.5 × 8 module under different conditions are listed in Table 2. It is evident that L_{eff} decreases with increasing liquid-phase velocity u_L and absorbent concentration but increases with increasing gas-phase velocity u_g. Similarly, Table 3 shows the results of L_{eff} in extra-flow 4 × 28 module.

Table 2. Effective fiber length (in mm) for CO_2 absorption by aqueous MEA solutions in extra-flow 2.5 × 8 module (L = 190 mm).

u_L (m s^{-1})	u_g = 0.041 m s^{-1}			u_g = 0.062 m s^{-1}			u_g = 0.124 m s^{-1}		
	0.005 M	0.01 M	0.1 M	0.005 M	0.01 M	0.1 M	0.005 M	0.01 M	0.1 M
7.96×10^{-3}	192.3	189.3	5.0	232.0	228.2	8.3	257.4	252.0	29.4
1.10×10^{-2}	153.9	146.9	2.6	196.3	193.4	4.0	241.8	238.2	12.0
1.59×10^{-2}	146.1	135.8	2.1	184.0	180.5	3.0	229.4	225.6	8.2
2.00×10^{-2}	141.9	126.6	1.8	177.8	174.9	2.4	225.0	221.9	6.1

Table 3. Effective fiber length (in mm) for CO_2 absorption by aqueous MEA solutions in extra-flow 4 × 28 module (L = 620 mm).

u_L (m s^{-1})	u_g = 0.041 m s^{-1}		u_g = 0.062 m s^{-1}		u_g = 0.124 m s^{-1}	
	0.005 M	0.1 M	0.005 M	0.1 M	0.005 M	0.1 M
7.96×10^{-3}	54.6	1.3	58.4	6.2	64.7	9.1
1.10×10^{-2}	43.7	0.7	48.8	1.2	61.0	3.1
1.59×10^{-2}	41.8	0.6	45.2	1.2	57.7	2.1
2.00×10^{-2}	41.0	0.5	43.5	1.2	56.6	1.6

Evidently, such a simplified model can predict a suitable membrane length of the fiber for desired CO_2 removal or estimate an appropriate absorbent concentration for fixed length of the fiber. Generally speaking, the knowledge of effective fiber length is important for economical applications of HFMC processes. The relationship among effective fiber length, gas-phase flow rate, and absorbent concentration for fixed emissive CO_2 concentration is crucial for the HFMC process to scale up.

5. Conclusions

The absorption of CO_2 from CO_2-N_2 mixtures using water and monoethanolamine (MEA) solution as absorbent liquids in hollow-fiber polypropylene membrane contactors has been experimentally and theoretically investigated. Through the use of the overall mass-transfer coefficients purely evaluated from physical absorption (i.e., water), a simplified model that considers mass balance equations and membrane non-wetting acceptably followed chemical absorption process (i.e., MEA); this is particularly true for a concentration of MEA lower than 0.05 M, where the standard deviation was less than 15%. The time changes of the gas-phase CO_2 concentration in the outlet of the module, as well as the gas-phase CO_2 concentration along the fiber within the module, could be obtained by iterative calculation. Model prediction of the effective length of the fiber, defined as the length from the inlet where the gas-phase CO_2 concentration reduced to zero, depended not only on the contact area of the module but also on the total length of the fiber. Although membrane wetting was more serious at higher MEA concentrations (e.g., 1.0 M), on average, model predictions still adequately described the dynamics of CO_2 absorption process in hollow-fiber membrane contactors.

Author Contributions: Conceptualization, R.-S.J.; methodology, M.L.T., C.H.N. and R.-S.J.; validation, K.-Y.C. and R.-S.J.; formal analysis, M.L.T., C.H.N. and K.-Y.C.; investigation, K.-Y.C.; data curation, M.L.T., C.H.N. and K.-Y.C.; writing—original draft preparation, M.L.T., C.H.N. and R.-S.J.; writing—review and editing, R.-S.J.; supervision, R.-S.J.; funding acquisition, R.-S.J. All authors have read and agreed to the published version of the manuscript.

Funding: This research was funded by the National Science and Technology Council, Taiwan, grant number 111-2221-E-182-002.

Institutional Review Board Statement: Not applicable.

Informed Consent Statement: Not applicable.

Data Availability Statement: The data presented in this study are available on request from the corresponding author.

Conflicts of Interest: The authors declare no conflict of interest.

List of Symbols

A_T = effective contact area (m^2)
C = concentration of components (mol m^{-3})
C_0 = initial CO_2 concentration in gas phase (mol m^{-3})
H = Henry's law constant of CO_2 (m^3 Pa mol^{-1})
J_A = flux of CO_2 (mol m^{-2} s^{-1})
K_L = overall mass-transfer coefficient based on liquid phase (m s^{-1})
k_{-1} = first-order rate constant for the reverse reaction defined in Equation (8) (m^3 mol^{-1} s^{-1})
k_2 = second-order rate constant for the forward reaction defined in Equation (8) (m^3 mol^{-1} s^{-1})
$k_{2,MEA}$ = second-order rate constant defined in Equation (8) (m^3 mol^{-1} s^{-1})
k_B = second-order rate constant for base B defined in Equation (9) (m^3 mol^{-1} s^{-1})
k_w = k_B when B is water (m^3 mol^{-1} s^{-1})
k_{MEA} = k_B when B is MEA (m^3 mol^{-1} s^{-1})
L = fiber length (mm)
L_{eff} = effective fiber length for CO_2 absorption (mm)
N_z = the number of grids in the computational domain in the axial direction
Q_L = volumetric flow rate of liquid phase (m^3 s^{-1})
r_A = rate of reaction between CO_2 and MEA defined in Equation (10) (mol m^{-3} s^{-1})
R_A = overall rate of CO_2 absorption (mol s^{-1})
R = gas constant (=8.314 J mol^{-1} K^{-1})
SD = standard deviation defined in Equation (13) (%)
u_g = linear flow velocity of gas phase (m s^{-1})
u_L = linear flow velocity of liquid phase (m s^{-1})
V_{shell} = volume of shell side (m^{-3})
z = axial direction of the fiber (m)
Subscripts
A = CO_2 gas
B = base (amine, H_2O, etc.)
g = CO_2 in gas phase
in = inlet
L = CO_2 in liquid phase
lm = logarithm mean
out = outlet
w = water

References

1. Desideri, U.; Paolucci, A. Performance modeling of a carbon dioxide removal system for power plants. *Energy Convers. Manag.* **1999**, *40*, 1899–1915. [CrossRef]
2. Scholes, C.A.; Kentish, S.E.; Stevens, G.W.; de Montigny, D. Comparison of thin film composite and microporous membrane contactors for CO_2 absorption into monoethanolamine. *Int. J. Greenhouse Gas Control* **2015**, *42*, 66–74. [CrossRef]
3. Chuah, C.Y.; Kim, K.; Lee, J.; Koh, D.Y.; Bae, T.H. CO_2 absorption using membrane contactors: Recent progress and future perspective. *Ind. Eng. Chem. Res.* **2019**, *59*, 6773–6794. [CrossRef]
4. Rangwala, H.A. Absorption of carbon dioxide into aqueous solutions using hollow fiber membrane contactors. *J. Membr. Sci.* **1996**, *112*, 229–240. [CrossRef]
5. Gabelman, A.; Hwang, S.T. Hollow fiber membrane contactors. *J. Membr. Sci.* **1999**, *159*, 61–106. [CrossRef]
6. Li, J.L.; Chen, B.H. Review of CO_2 absorption using chemical solvents in hollow fiber membrane contactors. *Sep. Purif. Technol.* **2005**, *41*, 109–122. [CrossRef]
7. Mansourizadeh, A.; Ismail, A.F. Hollow fiber gas-liquid membrane contactors for acid gas capture: A review. *J. Hazard. Mater.* **2009**, *171*, 38–53. [CrossRef]
8. Hoff, K.A.; Svendsen, H.F. Membrane contactors for CO_2 absorption–Application, modeling and mass transfer effects. *Chem. Eng. Sci.* **2014**, *116*, 331–341. [CrossRef]

9. Zhang, Z.; Yan, Y.; Zhang, L.; Chen, Y.; Ran, J.; Pu, G.; Qin, C. Theoretical study on CO_2 absorption from biogas by membrane contactors: Effect of operating parameters. *Ind. Eng. Chem. Res.* **2014**, *53*, 14075–14083. [CrossRef]
10. Li, M.H.; Lie, Y.C. Densities and viscosities of solutions monoethanolamine + *N*-methyldiethanolamine + water and monoethanolamine + 2-amino-2-methyl-1-propanol + water. *J. Chem. Eng. Data* **1994**, *39*, 444–447. [CrossRef]
11. Versteeg, G.F.; van Swaaij, W.P.M. Solubility and diffusivity of acid gases (CO_2, N_2O) in aqueous alkanolamine solutions. *J. Chem. Eng. Data* **1988**, *33*, 29–34. [CrossRef]
12. Song, J.H.; Park, S.B.; Yoon, J.H.; Lee, H. Densities and viscosities of monoethanolamine + ethylene glycol + water. *J. Chem. Eng. Data* **1996**, *41*, 1152–1154. [CrossRef]
13. Liao, C.H.; Li, M.H. Kinetics of absorption of carbon dioxide into aqueous solutions of monoethanolamine + *N*-methyldiethanolamine. *Chem. Eng. Sci.* **2002**, *57*, 4569–4582. [CrossRef]
14. Xu, S.; Wang, Y.W.; Otto, F.D.; Mather, A.E. Kinetics of the reaction of CO_2 with 2-amino-2-methyl-1-propanol solutions. *Chem. Eng. Sci.* **1996**, *51*, 841–850. [CrossRef]
15. Yeon, S.H.; Sea, B.; Park, Y.I.; Lee, K.H. Determination of mass transfer rates in PVDF and PTFE hollow fiber membranes for CO_2 absorptions. *Sep. Sci. Technol.* **2003**, *38*, 271–293. [CrossRef]
16. Wang, R.; Li, D.F.; Liang, D.T. Modeling of CO_2 capture by three typical amine solutions in hollow fiber membrane contactors. *Chem. Eng. Process.* **2004**, *43*, 849–856. [CrossRef]
17. Yeon, S.H.; Sea, B.; Park, Y.I.; Lee, K.S.; Lee, K.H. Adsorption of carbon dioxide characterized by using the absorbent composed of piperazine and triethanolamine. *Sep. Sci. Technol.* **2004**, *39*, 3281–3300. [CrossRef]
18. Kim, Y.S.; Yang, S.M. Absorption of carbon dioxide through hollow fiber membranes using various aqueous absorbents. *Sep. Purif. Technol.* **2000**, *21*, 101–109. [CrossRef]
19. Wang, R.; Zhang, H.Y.; Feron, P.H.M.; Liang, D.T. Influence of membrane wetting on CO_2 capture in microporous hollow fiber membrane contactors. *Sep. Sci. Technol.* **2005**, *46*, 33–40. [CrossRef]
20. Mavroudi, M.; Kaldis, S.P.; Sakellaropoulos, G.P. Reduction of CO_2 emission by a membrane contacting process. *Fuel* **2003**, *82*, 2153–2159. [CrossRef]
21. Chun, M.S.; Lee, K.H. Analysis on a hydrophobic hollow fiber membrane absorber and experimental observations of CO_2 removal by enhanced absorption. *Sep. Sci. Technol.* **1997**, *32*, 2445–2466. [CrossRef]
22. Li, K.; Teo, W.K. Use of permeation and absorption method for removal in hollow fiber membrane modules. *Sep. Purif. Technol.* **1998**, *13*, 79–88. [CrossRef]
23. Astarita, G. Carbon dioxide absorption in aqueous monoethanolamine solutions. *Chem. Eng. Sci.* **1961**, *16*, 202–207. [CrossRef]
24. Barth, D.; Tondre, C.; Delpuech, J.J. Stopped-flow investigations of the reaction kinetics of carbon dioxide with some primary and secondary alkanolamines in aqueous solutions. *Int. J. Chem. Kinetics* **1986**, *18*, 445–457. [CrossRef]
25. Paul, S.; Ghoshal, A.K.; Mandal, B. Removal of CO_2 by single and blended aqueous alkanolamine solvents in hollow-fiber membrane contactor: Modeling and simulation. *Ind. Eng. Chem. Res.* **2007**, *46*, 2576–2588. [CrossRef]
26. Al-Marzouqi, M.H.; El-Naas, M.H.; Marzouk, S.A.M.; Al-Zarooni, M.A.; Abdullatif, N.; Faiz, R. Modeling of chemical absorption of CO_2 in membrane contactors. *Sep. Purif. Technol.* **2008**, *59*, 286–293. [CrossRef]
27. Zhang, H.Y.; Wang, R.; Liang, D.T.; Tay, J.H. Modeling and experimental study of CO_2 absorption in a hollow fiber membrane contactor. *J. Membr. Sci.* **2006**, *279*, 301–310. [CrossRef]
28. Penttila, A.; Dell'Era, C.; Uusi-Kyyny, P.; Alopaeus, V. The Henry's law constant of N_2O and CO_2 in aqueous binary and ternary amine solutions (MEA, DEA, DIPA, MDEA, and AMP). *Fluid Phase Equil.* **2011**, *311*, 59–66. [CrossRef]
29. Li, L.; Maeder, M.; Burns, R.; Puxty, G.; Clifford, S.; Yu, H. The Henry coefficient of CO_2 in the MEA-CO_2-H_2O system. *Energy Procedia* **2017**, *114*, 1841–1847. [CrossRef]
30. Happel, L. Viscous flow relative to arrays of cylinders. *AIChE J.* **1959**, *5*, 174–177. [CrossRef]
31. Versteeg, G.F.; Swaaij, W.P.M. On the kinetics between CO_2 and alkanolamines both in aqueous and non-aqueous solution I. Primary and secondary amines. *Chem. Eng. J.* **1988**, *43*, 573–585. [CrossRef]
32. Blauwhoff, P.M.M.; Versteeg, G.F.; van Swaaij, W.P.M. A study on the reaction between CO_2 and alkanolamines in aqueous solutions. *Chem. Eng. Sci.* **1984**, *39*, 207–225. [CrossRef]
33. Barth, D.; Tondre, C.; Delpuech, J.J. Kinetics and mechanisms of the reactions of carbon dioxide with alkanolamines: A discussion concerning the cases of MDEA and DEA. *Chem. Eng. Sci.* **1984**, *39*, 1753–1760. [CrossRef]
34. Danckwerts, P.V. The reaction of CO_2 with ethanolamines. *Chem. Eng. Sci.* **1979**, *34*, 443–446. [CrossRef]